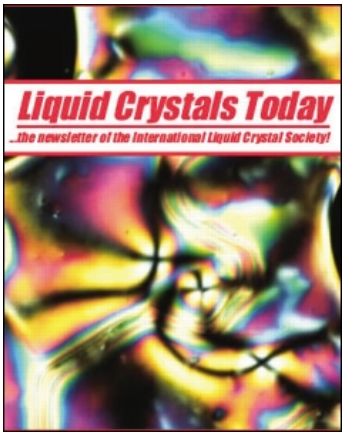

Liquid Crystals Today
Publication details, including instructions for authors and subscription information:
http://www.informaworld.com/smpp/title~content=t713681230

Liquid Crystals, the Visual System and Polarization Sensitivity

Nicholas W. Roberts[a]; Shelby Temple[b]; Theodore Haimberger[b]; Helen F. Gleeson[a]; Craig W. Hawryshyn[b]
[a] Department of Physics and Astronomy, Schuster Laboratory, University of Manchester, Manchester M13 9PL, UK [b] Department of Biology, University of Victoria, Victoria, British Columbia V8W 3N5, Canada

Online publication date: 19 May 2010

To cite this Article Roberts, Nicholas W. , Temple, Shelby , Haimberger, Theodore , Gleeson, Helen F. and Hawryshyn, Craig W.(2004) 'Liquid Crystals, the Visual System and Polarization Sensitivity', Liquid Crystals Today, 13: 2, 1 — 7
To link to this Article: DOI: 10.1080/14645180412331291861
URL: http://dx.doi.org/10.1080/14645180412331291861

Liquid Crystals Today, 2004, Vol. 13, No. 2, 1–7

Taylor & Francis
Taylor & Francis Group

Liquid Crystals, the Visual System and Polarization Sensitivity

NICHOLAS W. ROBERTS*, SHELBY TEMPLE†,
THEODORE HAIMBERGER†, HELEN F. GLEESON* and
CRAIG W. HAWRYSHYN†

*Department of Physics and Astronomy, Schuster Laboratory, University of Manchester, Manchester M13 9PL, UK
†Department of Biology, University of Victoria, P.O. Box 3020 STN CSC, Victoria, British Columbia V8W 3N5, Canada

We have examined the vertebrate visual system from a liquid crystalline perspective, with the aim of understanding the mechanisms responsible for polarization vision in vertebrates. Using a technique called micro-spectrophotometry (MSP), we show that the different types of light-sensitive cells in the retina absorb polarized light differently. Based on these measured geometries of absorbance, analytic solutions to Maxwell's equations using a 4×4 matrix technique demonstrate the possibility of intrinsic linear dichroism under axial illumination in those photoreceptors sensitive to polarized light. This provides a new mechanism for axial polarization sensitivity in vertebrate photoreceptors.

Introduction

Polarized light is an intrinsic element of the visual environment and recent research has described the ability of several species of vertebrate to both detect and interact with their perception of the surrounding polarized light field [1–7]. Although we understand that different types of photoreceptor (the light-sensitive cells of the retina) are sensitive to polarized light in different ways, the bio-physical mechanism by which the plane of polarization is analysed is still not well understood [4, 7]. But what does this have to do with liquid crystals? Within the retina there are two different types of photoreceptor - rods and cones - with both types of cell containing model examples of a lamellar liquid crystal phase. The part of the cell that contains the visual pigment is made up of several hundred lipid bi-layers. This is illustrated in Figure 1 with an electron micrograph and schematic diagram of a rod photoreceptor. An opsin protein and vitamin A derivative chromophore form the visual pigment (called rhodopsin) with each molecule spanning the individual bi-layers. As such, the photoreceptor structure is almost directly analogous to a guest-host liquid crystal device, the chromophore orientated by the liquid crystal host and maximally absorbing light polarized linearly to the chromophore's long axes. However, in this case the long axis of the chromophore is orientated perpendicular to the director. It has been assumed that in general, vertebrate photoreceptors are not linearly dichroic to polarized light propagating along the long axis of the cell [5, 8, 9] (the physiological illumination geometry). This is thought to be due to rotational diffusion of the rhodopsin within the outer-segment membranes [10, 11]. However, diffusion measurements have been reported only for non-polarization sensitive rod photoreceptors, and it is well known that in vertebrates, polarization sensitivity is mediated exclusively by the ultra-violet, middle and long spectral classes of cone [1, 2].

Correspondence should be addressed to N. W. R. (email: nickr@fs3.ph.man.ac.uk).

Experimental Absorbance Measurements

Microspectrophotometry (MSP) is a technique that measures the transverse spectral absorbance of single photoreceptors [12–17], and due to the dichroic nature of the chromophore, further information can be obtained regarding spatial degree of absorbance by linearly polarizing the measurement beam [18]. Measures of absorbance parallel and perpendicular to the long axis of the outer segment have been used extensively to measure dichroic ratios [8, 12, 13]. These are similar to dichroic ratio measurements made in guest host liquid crystal systems. In this investigation, we have measured the transverse absorbance of all spectral classes of photoreceptors in coho salmon (*Oncorhynchus kisutch*), a species with known polarization sensitivity, as a function of the angle between the E-vector and the short axis of the photoreceptor outer segment. Throughout this work, this angle will be referred to as the polarization angle, ϕ. An illustration of this technique is given in Fig. 2(a), where

Liquid Crystals Today ISSN 1464-5181 online © 2004 Taylor & Francis Ltd
http://www.tandf.co.uk/journals
DOI:

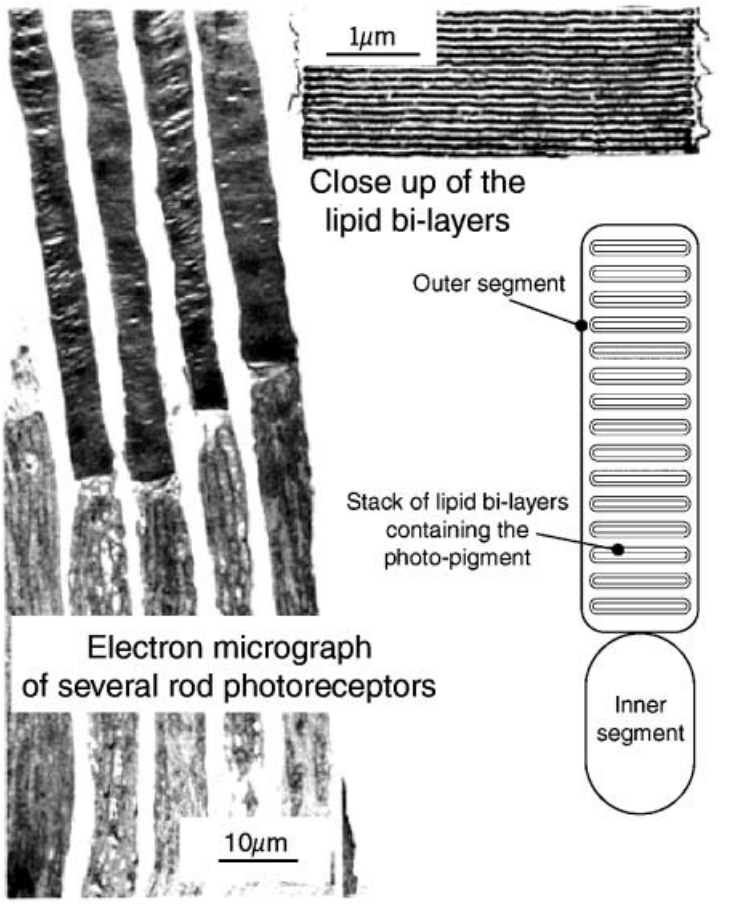

Figure 1. Electron micrograph and schematic diagram of a rod photoreceptor and its outer segment [adapted from 19].

different E-vectors, labeled by the polarization angle, are incident (z direction) on a photoreceptor. Polarization absorbance measurements were made for $\phi = 0^\circ$, 20°, -20°, 10°, -10°, 0° and the sequence of measurements was consistently as stated. An inherent limitation of multiple measurements of absorbance in photoreceptors is photobleaching [19]. To minimize this effect, our work utilized a unique CCD PMSP system [17]. A calibration experiment proved that due to the system's rapid full spectrum acquisition, eight consecutive spectra could be consistently measured before the value of the maximum absorbance dropped below 2 S.D. of the initial level. Moreover, the sequence of measurements facilitated the comparison of the spectra at 0°. If the final values of maximum absorbance were more than 2 S.D. below the initial value, the photoreceptor was deemed bleached or moved and the data set rejected. As a further control, a set of absorbance measurements were made in the stated order from both a rod and MWS cone photoreceptor after their respective outer segments had been bleached. The results of this test showed that the bleached baseline absorbance measurement remained constant regardless of the polarization angle. The sequence also proved that greater values of the maximum absorbance at $\phi = \pm 10^\circ$ or $\pm 20^\circ$ could not be a result of bleaching. A typical absorbance spectrum (black curve) from a mid wavelength-sensitive cone is presented in Figure 2(b) together with the fit to the data (grey curve). Data were first smoothed using a 25 point adjacent averaging then fitted using a non-linear least squares routine utilizing the weighted A1/A2 averaged Govadovskii [16] template. Two typical polarization absorbance data sets deduced from the fits are shown in Figures 2(c) and 2(d) for a rod and long wavelength-sensitive cone respectively. Here, there is a difference in the polarization angle that yields the greatest value of absorbance.

This effect is emphasized by Figures 3(a–e), which present typical maximum values of absorbance for the fits as a function of ϕ. The curves in the Figures 3(a–e) are the fitted theoretical absorbance [20].

$$a_i = -\log_{10}\left(\cos^2(\phi - \Phi_i)10^{-a_{\|}} + \sin^2(\phi - \Phi_i)10^{-a_{\perp}}\right), \quad (1)$$

where i denotes the spectral class of photoreceptor and a_i is the measured absorbance. $a_{\|}$ and $a_{\perp}$ are the

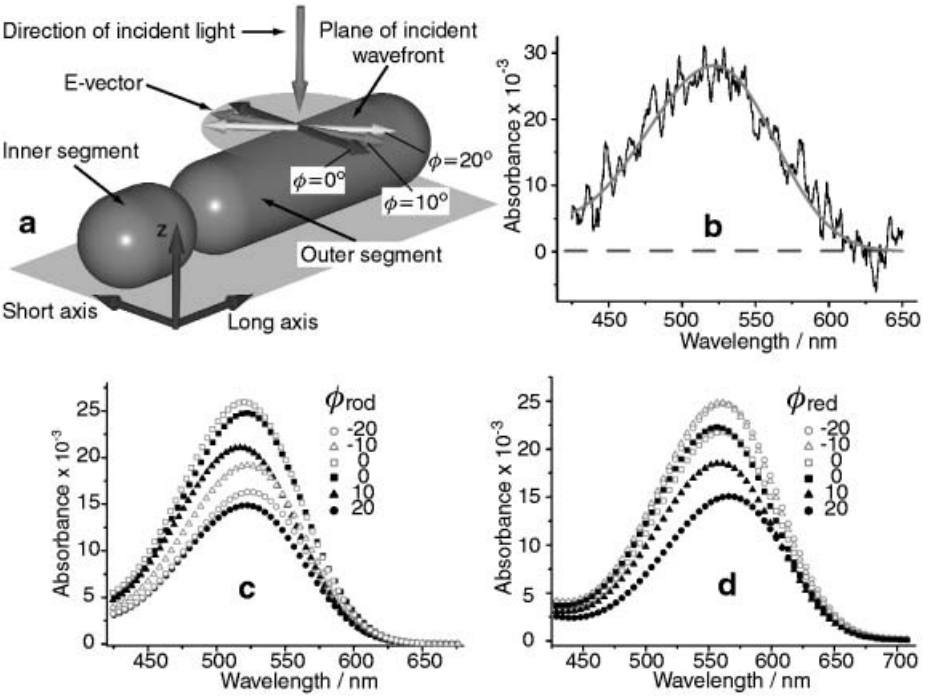

Figure 2. The technique of polarization microspectrophotometry and associated experimental results. (**a**) A schematic diagram of the inner and outer segments of a vertebrate photoreceptor. Linearly polarized light is shown in the experimental measurement geometry incident on the outer segment, with the different e-vectors corresponding to the labelled polarization angles, ϕ. (**b**) A typical experimental absorbance spectrum obtained from a mid wavelength-sensitive cone. (**c**–**d**) Sets of fitted spectral absorbance data for a rod and long wavelength-sensitive cone photoreceptor using the weighted A1/A2 Govardovskii template [16]. The maximum positions of absorbance are, $\Phi = 0^\circ$ and between -10° to -20° for the rod and cone respectively. In both (**c**) and (**d**) the legend indicates ϕ.

absorbance parallel and perpendicular to the short axis of the outer segment respectively. Φ_i is the polarization angle corresponding at maximum absorbance. The values of Φ_i from Figures 3(a–e) are presented in Table 1. Although Φ_i is centered around 0° for the rod, in the four spectral classes of cone, it deviates significantly from 0°.

Figure 4 illustrates the distributions in Φ for all the measured rods and cones. A standard parametric (ANOVA) test was used to determine whether the mean value of the distribution of Φ for the rods, μ_{rod}, was significantly different from the mean value of Φ for the cones, μ_{cone}. The results of the test do indeed reveal a statistically significant difference between μ_{rod} and μ_{cones} ($F_{1,\ 78} = 76.802$, $P < 0.001$).

A Tukey HSD multiple comparison was also used to investigate significant differences in the mean values of Φ between each spectral class of photoreceptor. The results of this test are presented in Table 2 and reveal that μ_{rod} is significantly lower than $\mu_{UVS\ cone}$, $\mu_{MWS\ cone}$ and $\mu_{LWS\ cone}$ (in all cases $P < 0.001$). There is no significant difference between the mean values of Φ between different spectral classes of cone ($P \geq 0.601$) and between μ_{rod} and $\mu_{SWS\ cone}$ ($P \geq 0.289$). However, it should be noted that the sample sizes for the UVS and SWS cone measurements were $n = 4$ and $n = 3$ respectively. Consequently, the powers of the tests for the comparisons between the UVS and SWS cones and other photoreceptors are < 0.2. This makes it difficult to assess the real significance of these statistical data for the UVS and SWS cones as there is a $> 80\%$ chance of Type II error. However, the measurements of the UVS and SWS cones did reveal that Φ was tilted to a greater angle in these cones than for any of the more numerous rod measurements. This implies that the UVS and SWS classes have similar optical properties to the MWS and LWS cones measured.

Underlying Optical Structure

The slight tilt of the chromophore main absorption dipole within the opsin protein [12, 21, 22] cannot account for this result. For any chromophore tilt angle under 45°, rotational diffusion will average the absorbance, ensuring that Φ would be perpendicular to the bi-layer director. There are, however, two plausible explanations that account for the tilted values of Φ. Either the membranes are tilted with respect to the axes of the outer segments, or the director

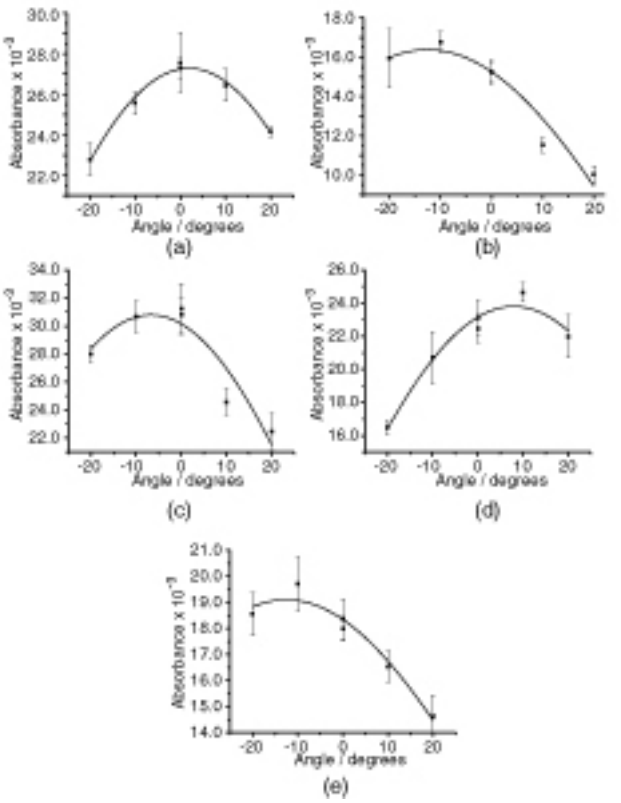

Figure 3. Absorbance values as a function of polarization angle, ϕ. Points correspond to experimental data, the line corresponds to numerical fit as described in equation 1. (**a**) In the rod, the angle of maximum absorbance, Φ, is parallel to the minor axis of the outer segment. In (**b**) the UV-sensitive cone, (**c**) the short wavelength-sensitive cone, (**d**) the mid wavelength-sensitive cone and (**e**) the long wavelength-sensitive cone, Φ deviates from the 0°.

within the membranes is tilted with respect to the layer normal. In *Anchoa mitchilli* and *A. hepsetus*, it is known that the plane of the membranes within the polarization–sensitive cones are orientated parallel to the long axis of the outer segments [4]. However, this observation represents a unique example. To date no published electron microscopy data have been presented as evidence for a consistent tilt of the membranes within the outer segments of polarization-sensitive

Table 1. Polarization angles of maximum absorbance, Φ, from typical single photoreceptors in each spectral class as illustrated in Figures 3(a–e).

Photoreceptor Type	Φ/°
Rod	2 ± 1
UV-sensitive cone	12 ± 2
Short wavelength-sensitive cone	7 ± 3
Mid wavelength-sensitive cone	8 ± 2
Long wavelength-sensitive cone	13 ± 3

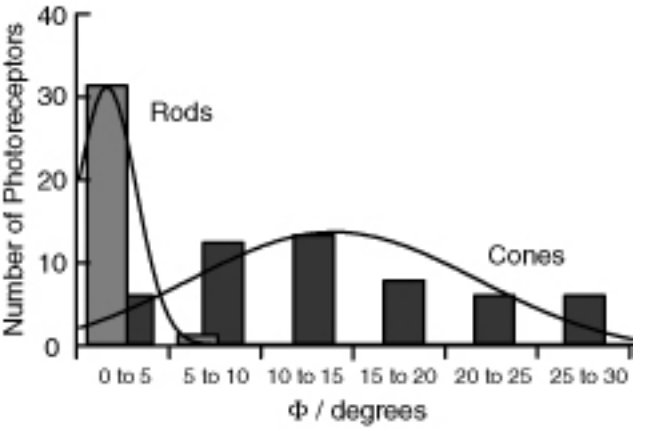

Figure 4. Illustrates the mean value in Φ for all the measured rods and cones.

photoreceptors in salmonids or any other taxonomic group. The second possibility relates to the known differences in the physiological structure of rods and cones. While the membranous discs containing the photo-pigment in rods are not connected to the outer cell membrane, the double membranes of cones are evaginations and continuation of the outer cell membrane [19]. It has been shown that rod membranous discs and the outer cell membrane differ in both physical and chemical properties [19]. For example, significantly higher levels of cholesterol occur in the outer cell membrane compared to the inter rod discs [23]. Furthermore, increased levels of cholesterol are known to cause a director tilt within a lipid bi-layer [24–26]. It is therefore reasonable to suggest that the tilted position of maximum absorbance in the cones is a direct result of the different photoreceptor structures and the physical and compositional differences therein.

Modeling

A clear limitation in this investigation of polarization vision is that under natural conditions photoreceptor illumination is axial and not transverse as in the experimental geometry used in MSP. To investigate the effect of the measured difference between the rods and cones under axial illumination, analytic solutions to Maxwell's equations were derived for the tilted and non-tilted outer segment structures. The model used was based on a 4×4 matrix approach, similar to the Berreman method, and commonly used in investigating the selective reflection properties of chiral liquid crystals [27]. The formulation of a complex dielectric tensor for the system accounts for all aspects of the complex refractive indices, chromophore tilt [12, 21, 22], rotational diffusion [10, 11], rotational degree of freedom of the photoreceptor as a whole and the tilt

Table 2. Probability values from a comparison (Tukey Test)[a] of mean values of Φ between all spectral classes of photoreceptors.

	UVS cone (n = 4)	SWS cone (n = 3)	MWS cone (n = 22)	LWS cone (n = 19)	Rod (n = 32)
UVS cone		0.601	0.990	0.982	0.000
SWS cone			0.643	0.695	0.289
MWS cone				1.000	0.000
LWS cone					0.000
Rod					

[a]The statistical test was performed using SYSTAT 9.0.

of the plane of absorbance within the outer segments of the cones. Calculations of the absorbance spectra of two axial orthogonal polarized beams incident on a rod and cone outer segment are presented in Figures 5(a) and 5(b) respectively. It can be seen that the tilt of the plane of absorbance causes the system to be intrinsically linearly dichroic. Figure 5(c) illustrates this effect more clearly. The absorbance is plotted at λ_{max} as a function of the rotational angle of linear incident polarization. Here 0° corresponds to the E-vector parallel to the plane of incidence containing the director. The results in Figure 5(c) show that there is an approximate 10% difference between the absorbance of orthogonal axially propagating linear polarized light.

Conclusion

To our knowledge, this is the first report of significant differences between the way rods and cones photoreceptors absorb linearly polarized light. The results strongly suggest that the position of maximum absorbance in cones is tilted with respect to the primary axes of the cell. A plausible hypothesis was presented for the basis of this tilt, based upon structural and compositional differences resulting in the different optical properties. Finally, analytic solutions to Maxwell's equations were deduced to investigate the effect of the tilt upon the absorbance under axial illumination of the outer segment. The results of this part of the study suggest the possibility of axial dichroism within the cone photoreceptors that specifically mediate polarization vision in salmonid fish. However, further experimental work is required to both directly measure differential axial polarization absorbance and to study the implications of the interaction with other possible mechanisms of polarization sensitivity [13]. In general, it is possible that with the correct orientation of this optical geometry in the retina, axial dichroism of vertebrate photoreceptors may provide a similar unifying mechanism of polarization sensitivity that exists between many species of invertebrate.

Methods

Animals

Coho salmon (*Oncorhynchus kisutch*) were acquired from the Robertson Creek Hatchery, Port Alberni, BC. The fish were maintained on a 12:12h light:dark cycle and at a temperature of 15°C. All fish were parr, with a

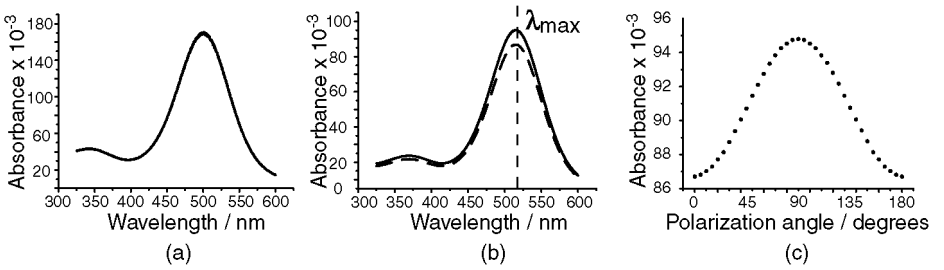

Figure 5. Calculated solutions to Maxwell's equations for an axially illuminated rod and cone photoreceptor. Defining $n_{external}$ as the refractive index of the surrounding cytoplasm and $n_{\parallel}$ and $n_{\perp}$ as the anisotropic refractive indices parallel and perpendicular to the director of the internal membranes, the parameters used for this calculation were: Refractive indices [28, 29] $n_{external} = 1.365$, $n_{\parallel} = 1.486$, $n_{\perp} = 1.464$, the extinction coefficient was based on the wavelength dependence profiles of Stavenga and Barneveld [30], the chromophore tilt angle [12, 21] = 16°, the tilt of the absorbance ellipsoid = 15°, the outer segment length = 10 μm and the bi-layer thickness = 120Å. Two orthogonal absorbance curves (a) for a rod and (b) for an LWS cone. The solid and dashed correspond to the E-vector parallel and perpendicular to the plane of incidence that contains the director. In (a) both curves are indistinguishable illustrating no polarization discrimination. In (b) there is a noticeable difference between polarizations across the absorption band. The modulation in the absorbance at λ_{max} is shown in (c). An approximately 10% difference in absorbance as a function of E-vector orientation illustrates the intrinsic axial polarization sensitivity of the outer segment.

mean ($\pm$1. S.D.) size and weight of 9.3$\pm$1.7cm and 10.2$\pm$3.2g respectively. Care and handling procedures were in accordance with the Canadian Council on Animal Care guidelines.

Polarization microspectrophotometry

Spectral absorbance measurements were made from the photoreceptors of 18 fish. The analysis is based on the measurements from n=32 rods and n=48 cones that fitted the aforementioned criteria for acceptable absorbance spectra relative to polarization angle. Sample sizes were calculated using a power analysis to investigate a 10° minimum detectable difference between the angles of maximum absorbance of different classes of photoreceptor. Detailed descriptions of the MSP protocols and sample preparations have been described elsewhere [17]. A modification to this protocol was the inclusion of a Glan-Thompson polarizer immediately preceding the condenser assembly. The axis of the polarizer was calibrated with respect to the image orientation on the computer, allowing digital calculation ($\pm$1°) of the required polarization measurement angle. Spectra acceptance criteria were used as documented by Hawryshyn *et al.* [17] and as described above with relation to the sequence of measurements.

Acknowledgements

The authors wish to thank Robertson Creek Hatchery for supplying the experimental animals and J. Lydon for very helpful discussions at the outset of this study. This research was supported by a travel fellowship to N.W.R. from the Journal of Experimental Biology and operating and equipment grants to H.F.G. from the Engineering and Physical Sciences Research Council and to C.W.H. from the Natural Sciences and Engineering Research Council of Canada.

References

[1] Parkyn, D. C., and Hawryshyn, C. W., 2000, Spectral and ultraviolet-polarization sensitivity in juvenile salmonids: a comparative analysis using electrophysiology. *J. Exp. Biol.*, **203,** 1173–1191.

[2] Coughlin, D. J., and Hawryshyn, C. W., 1995, A cellular basis for polarized-light vision in rainbow trout. *J. Comp. Physiol. A*, **176,** 261–272.

[3] Roberts, N. W., Temple, S. E., Haimberger, T. J., Gleeson, H. F., and Hawryshyn, C. W., 2004, Differences in the optical properties of vertebrate photoreceptor classes leading to axial polarization sensitivity. *J. Opt. Soc. Am. A,* **21**(3), 355–345.

[4] Fineran, B. A., and Nicol, J. A. C., 1978, Studies on the photoreceptors of *Anchoa mitichilli* and *A. hepsetus* (Engranlidae) with particular reference to the cones. *Philos. Trans. R. Soc. Lond. Ser. B*, **283,** 25–60.

[5] Waterman, T. H., 1981, Polarization sensitivity. *Handbook of Sensory Physiology VII/6B* Springer-Verlag Berlin, 430–435.

[6] Flamerique, I. N., and Browman, H. I., 2001, Foraging and prey-search behaviour of small juvenile rainbow trout (*Oncorhynichus mykiss*) under polarized light. *J. Exp. Biol.*, **204,** 2415–2422.

[7] Flamarique, I. N., Hawryshyn, C. W., and Harosi, F. I., 1998, Double cone internal reflection as a basis for polarization detection in fish. *J. Opt. Soc. Am. A*, **51,** no. 2, 349–358.

[8] Snyder, A. W., 1979, Physics of Vision in compound eyes. *Handbook of Sensory Physiology VII/6A*. Ed. Autrum, H., Springer Verlag, Berlin, 284–285.

[9] Land, M. F., and Nilsson, D.-E., 2002, Light and vision. *Animal Eyes*. Oxford University Press, 1st edition, 29–31.

[10] Brown, P. K., 1972, Rhodopsin rotates in the visual receptor membrane. *Nature New Biology*, **236,** 35–38.

[11] Cone, R. A., 1972, Rotational diffusion of rhodopsin on the visual receptor membrane. *Nature New Biology*, **236,** 39–43.

[12] Liebman, P. A., 1962, In situ microspectrophotometric studies on the pigments of single retinal rods. *Biophys. J.*, **2,** 161–178.

[13] Harosi, R. E., and MacNichol, E. F., Jr., 1974, Dichroic microspectrophotometer: a computer assisted, rapid, wavelength scanning photometer for measuring the linear dichroism of single cells. *J. Opt. Soc. Amer.*, **64,** 903–918.

[14] Loew, E. R., and Dartnall, H. J. A., 1976, Vitamin A_1/A_2-based visual pigment mixtures in cones of the rudd. *Vision Res.*, **16,** 891–896.

[15] Bowmaker, J. M., 1984, Microspectrophotometry of vertebrate photoreceptors. *Vision Res.*, **24,** 1641–1650.

[16] Govardovskii, V. I., Fyhrquist, F., Reuter, T., Kuzmin, D. G., and Donner, K., 2000, In search of the visual pigment template. *Vis. Neuro.*, **17,** 509–528.

[17] Hawryshyn, C. W., Haimberger, T. J., and Deutschlander, M. E., 2001, Microspectrophotometric measurements of vertebrate photoreceptors using CCD-based detection technology. *J. Exp. Biol.*, **204,** 2431–2438.

[18] Schmidt, W. J., 1938, Polarizationsoptische analyse eiens Eiweiß-lipiod-systems, erläutert am Außengield der sehzellen. *Kolliodzeitschrift*, **85,** 137–148.

[19] Cohen, A. I., 1972, Rods and Cones. *Handbook of Sensory Physiology VII/2*. Ed. Fuortes, M. G. F., Springer Verlag, Berlin, 63–110.

[20] Born, M., and Wolf, E., 1999, *Principles of Optics*. Cambridge University Press, 7th Edition, 218–219.

[21] Harosi, F. I., and Malerba, F. E., 1975, Plane polarized light in microspectrophotometry. *Vision Res.*, **15,** 379–388.

[22] Gröbner, G., Burnett, C. G., Choi, A., Mason, J., and Watts, A., 2000, Observations of light-induced structural changes of retinal within rhodopsin. *Nature*, **405,** 810–813.

[23] Boesze-Battaglia, K., and Schimmel, R. J., 1997, Cell membrane lipid composition and distribution: Implications for cell function and lessons learned from photoreceptors and platelets. *J. Exp. Biol.*, **200,** 2927–2936.

[24] Murari, R., Murari, M. P., and Baumann, W. J., 1986, Sterol orientations in phosphatidycholine liposomes as determined by deuterium NMR. *Biochemistry*, **25,** 1062–1067.

[25] McIntosh, T. J., 1973, The effect of cholesterol on the structure of phosphatidycholine bilayers. *Biochim. et Biophys. Acta.*, **513,** 43–58.

[26] Brzustowicz, M. R., Stillwell, W., and Wassall, S. R., 1999, Molecular organization in polyunsaturated phospholipid membranes: a solid state ^{2}H NMR investigation. *FEBS Letters*, **451,** 197–202.

[27] Berreman, D., 1972, Optics in stratified and anisotropic media: 4×4-matrix formulation. *J. Opt. Soc. Amer.*, **62,** 502–10.

[28] Liebman, P. A., Jagger, W. S., Kaplan, M. W., and Bargoot, F. G., 1974, Membrane structure changes in rod outer segments associated with rhodopsin bleaching. *Nature*, **251,** 31–36.

[29] Israelchvili, J. N., Sammut, R. A., and Snyder, A. W., 1976, Birefringence and dichroism of photoreceptors. *Vision Res.*, **16,** 47–52.

[30] Stavenga, D. G., and van Barneveld, H. H., 1975, On dispersion in visual photoreceptors. *Vision Res.*, **15,** 1091–1095.